Appl Microbiol Biotechnol (2015) 99:97–107
DOI 10.1007/s00253-014-5929-7

ENVIRONMENTAL BIOTECHNOLOGY

Modeling the effects of biomass accumulation on the performance of a biotrickling filter packed with PUF support for the alkaline biotreatment of dimethyl disulfide vapors in air

Luis Arellano-García · Antonio D. Dorado · Axayacatl Morales-Guadarrama · Emilio Sacristan · Xavier Gamisans · Sergio Revah

Received: 5 May 2014 / Revised: 30 June 2014 / Accepted: 1 July 2014 / Published online: 25 July 2014

Abstract Excess biomass buildup in biotrickling filters leads to low performance. The effect of biomass accumulation in a biotrickling filter (BTF) packed with polyurethane foam (PUF) was assessed in terms of hydrodynamics and void space availability in a system treating dimethyl disulfide (DMDS) vapors with an alkaliphilic consortium. A sample of colonized support from a BTF having been operating for over a year was analyzed, and it was found that the BTF void bed fraction was reduced to almost half of that calculated initially without biomass. Liquid flow through the examined BTF yielded dispersion coefficient values of 0.30 and 0.72 $m^2\ h^{-1}$, for clean or colonized PUF, respectively. 3D images of attached biomass obtained with magnetic resonance imaging allowed to calculate the superficial area and the biofilm volume percentage and depth as 650 $m^2\ m^{-3}$, 35 %, and 0.6 mm respectively. A simplified geometric approximation of the complex PUF structure was proposed using an orthogonal 3D mesh that predicted 600 $m^2\ m^{-3}$ for the same biomass content. With this simplified model, it is suggested that the optimum biomass content would be around 20 % of bed volume. The activity of the microorganisms was evaluated by respirometry and the kinetics represented with a Haldane equation type. Experimentally determined parameters were used in a mathematical model to simulate the DMDS elimination capacity (EC), and better description was found when the removal experimental data were matched with a model including liquid axial dispersion in contrast to an ideal plug flow model.

Keywords Biotrickling filter · Magnetic resonance imaging · Biofilm · Modeling · Dimethyl disulfide · Liquid dispersion

Electronic supplementary material The online version of this article (doi:10.1007/s00253-014-5929-7) contains supplementary material, which is available to authorized users.

L. Arellano-García
Departamento de Ingeniería de Procesos e Hidráulica, UAM Iztapalapa, San Rafael Atlixco 186, Col. Vicentina, Iztapalapa, Mexico City 09340, Mexico

A. D. Dorado · X. Gamisans
Departamento de Ingeniería Minera y Recursos Naturales, UPC, Av. Bases de Manresa 61-73, 08242Manresa Barcelona, Spain

A. Morales-Guadarrama · E. Sacristan
Departamento de Ingeniería Eléctrica, UAM Iztapalapa, San Rafael Atlixco 186, Col. Vicentina, Iztapalapa, Mexico City 09340, Mexico

A. Morales-Guadarrama · E. Sacristan
Centro Nacional de Investigación en Imagenología e Instrumentación Médica, UAM Iztapalapa, San Rafael Atlixco 186, Col. Vicentina, Iztapalapa, Mexico City 09340, Mexico

S. Revah (✉)
Departamento de Procesos y Tecnología, UAM Cuajimalpa, Artificios 40, Col. Hidalgo, Álvaro Obregón, Mexico City 01120, Mexico
e-mail: srevah@xanum.uam.mx

Introduction

Odor control is a priority in populated areas because of public complaints near emission sources or greater environmental awareness reflected in stronger air quality regulation. In this regard, the efficiency of biological processes for the treatment of malodorous sulfur compounds, such as hydrogen sulfide, mercaptans, inorganic, and organic sulfides, has been thoroughly tested (Smet and Van Langenhove 1998; González-Sánchez et al. 2008; Ramírez et al. 2011; Estrada et al. 2012; Silva et al. 2012).

In biofilters and biotrickling filters, odor causing pollutants in air are transferred to an active biofilm where they are transformed to non-odorous substances while more biomass is produced. Initially, and with adequate environmental

conditions including active biomass, sufficient nutrients and well-distributed water flow over the packing biomass growth would be expected to occur by the colonization of all the superficial area of the support. The extended thin layer enhances the contaminant transport to the interior of the biofilm, which remains completely active. Nonetheless, sustained biomass accumulation in BTF packing leads initially to reduced efficiency and ultimately to shut down due to different factors. Firstly, at micro and mesoscopic level, the increase in the biofilm depth provokes that the innermost part becomes inactive (by either substrate or oxygen limitation). Secondly, irregularities in liquid and gas flows are developed from biofilm growth leading to fluctuations in the velocity profiles. At macroscopic scale, biomass accumulation induces the narrowing of air and liquid passages with consequent overall residence time reduction and increased pressure drop (Alonso et al. 1996; Trejo-Aguilar et al. 2005; Dorado et al. 2012).

Assessing biomass accumulation in biotrickling filters may be accomplished at both scales by diverse methodologies. At small scale, microscopy is often utilized (De Beer and Stoodley 2006) but also a medical analysis technique such as magnetic resonance imaging (MRI) can be used to examine the accumulation of biomass and the biofilm structure as has been recently reviewed by Neu et al. (2010). MRI generates 3D images of the attached biofilm which, through further image processing, can be employed to obtain quantitative data such as the interfacial area and the volume. Deshusses et al. (1998) determined interfacial area and biofilm thickness in BTF and biofilter beds by computerized axial tomography reporting that the superficial area was higher than expected and it was related to biofilm roughness and concluded that further analyses of other supports at different void fractions were needed.

At the reactor (macroscopic) dimension, pressure drop is usually evaluated as a response to biomass growth (or accumulated byproducts such as elemental sulfur, EPS, etc.). Further assessment at this scale includes the evaluation of the residence time distribution technique (RTD), which has been used for characterizing the hydrodynamics in biotrickling filters (Iliuta et al. 2002; Trejo-Aguilar et al. 2005; Sharvelle et al. 2008a). It is often considered that the liquid movement through a porous bed occurs by an ideal plug flow pattern. Nonetheless, some preferential channels or stagnant zones may arise as a consequence of packing structure and heterogeneity of biofilm growth, thus giving place to axial dispersion. In this sense, RTD analysis provides a measure of liquid dispersion for circulating fluids in packed beds. Many models and correlations accounting for axial dispersion in trickle-bed reactors have been described (Herskowitz and Smith 1983; Gianetto and Specchia 1992; Levenspiel 1998; Delgado 2006) with the piston dispersion model being the simplest and the more easily used in design. Nevertheless, the application of these expressions in modeling biotrickling filters is not common.

To date, only a few models include liquid dispersion to simulate gas treatment performance in biofilters and biotrickling filters (Zarook et al. 1998; Iliuta et al. 2002; Sharvelle et al. 2008b). Some other includes interesting analyses through biomass growth functions to predict its influence on the biofiltration process (Alonso et al. 1996; Alonso et al. 1998; Iliuta et al. 2002). However, these models were focused on packing particles with relatively simple geometries. Therefore, further studies are needed to evaluate hydrodynamic features of recently used packings, such as open pore polyurethane foam (PUF), coupled with biofilm buildup to simulate their effects over the gas treatment in biotrickling filters.

The aim of the present work was to examine the biomass accumulation effects over a long-term operated BTF hydrodynamics and performance. This objective was attained by assessing the biological intrinsic kinetics of the biofilm, by evaluating the available space and interfacial area for gas treatment in the BTF bed packed with open polyurethane foam through advanced imaging techniques and by simulating biofiltration performance using a mathematical model. Furthermore, a geometric model consisting in an orthogonal 3D mesh allowed representing the complex porous structure of PUF and predicting how the superficial area is affected as biomass increases and other hydrodynamic phenomena, such as reduced residence time or increased water hold-up are altered.

Materials and methods

Biotrickling filter

A squared column (0.08×0.08 m) BTF with four separated modules (height=0.12 m each) and five ports to sample gas or liquid (Fig. 1a) was used. It contained a total of 48 PUF cubes (0.04×0.04×0.04 cm) as carrier material. Superficial area for this specific PUF is 480 $m^2\ m^{-3}$ according to the manufacturer. The apparent density and porosity were determined in the laboratory and found to be 21 and 0.98 kg m^{-3}, respectively. Colonized PUF cubes were extracted from a previous alkaline BTF that was operated for more than a year degrading efficiently DMDS concentrations below 140 ppmv with 40 s of empty bed gas residence time, where biofilm was well developed in all the support. Information about the original consortium, mineral medium, and long-term gas treatment performance can be found elsewhere (Granada et al. 2009; Arellano-García et al. 2012). The gas inlet and outlet were positioned in such a way that the BTF could operate either counter-current or in parallel flow mode. The BTF was provided with a spray nozzle that distributes the liquid uniformly over the transversal area. The liquid volume at BTF bottom (V_{LRES}) was 0.8 L. The gas and liquid flows (Q_G and Q_L) were set at 0.27 and 0.04 $m^3\ h^{-1}$, respectively, to have a gas residence time of 40 s and linear velocities of gas (u_G) and liquid (u_L) of 42.0 and

6.5 m h^{-1}. The pressure drop for the gas stream was measured with a U tube manometer filled with water.

Intrinsic biological kinetics determination

Effective degradation rates without mass transfer effects were determined for biomass in a liquid phase respirometer, which consisted of a jacketed 2.6 mL glass chamber equipped with magnetic agitation, temperature control at 30° C, and a polarographic oxygen probe (YSI 5300A, USA). Biofilm samples were extracted from colonized PUF and milled in a glass pestle tissue grinder to eliminate macroscopic granules. The resultant slurry was washed twice with mineral medium to remove DMDS and then centrifuged to have a suspension which was used to evaluate biomass concentration in the biofilm by protein content. The respirometer was filled in batches with air-saturated alkaline mineral medium, a specific volume of biomass suspension and pulses of a concentrated DMDS aqueous solution. Specific oxygen consumption was registered as a function of DMDS and biomass protein concentration. The reaction rate of DMDS was evaluated based on biotic oxygen uptake rate and the oxidation stoichiometry reported by Smith and Kelly (1988) as shown in Eq. 1. Biological kinetics was estimated by minimizing the squared error between data from respirometry tests and the predictions of a Haldane type reaction model with inhibition by substrate.

$$CH_3{-}S{-}S{-}CH_3 + 6.5\,O_2 \rightarrow 2\,CO_2 + 2\,H_2SO_4 + H_2O \quad (1)$$

Trickling liquid flow pattern description

To characterize the liquid flow through the BTF, the liquid residence time distribution (RTD) technique was used. Dextran blue was utilized as tracer for the liquid stream as it is stable in time and pH, and its high molecular weight (approximate 20,000 g mol^{-1}) hinders absorption in the biofilm and packing material. Tracer pulses volume was in all cases 4 mL with a concentration of 10 g L^{-1}. The pulses were injected into the liquid stream through a septum located upstream just before the spray nozzle. Liquid samples were collected at intervals between 4 and 10 s, and their absorbance was measured within 1 h. The BTF dynamic liquid hold-up was obtained by measuring the liquid volume drained after 15 min of stopping gas and liquid flows.

The dispersed plug flow model equation for closed vessels (Eq. 2) was utilized to fit the experimental RTD curves and to determine dispersion coefficient values, as suggested by Levenspiel (1998) when the multiple samples method for collecting the tracer is used.

$$2\frac{D_{disp}}{u_L\,F} - 2\left(\frac{D_{disp}}{u_L\,F}\right)^2\left(1 - e^{-uL/D_{disp}}\right) - \frac{\sigma^2}{\underline{t}^2} = 0 \quad (2)$$

Where σ (h) is the time distribution variance of data, (h) flowing liquid average residence time, u_L (m h^{-1}) liquid superficial velocity, D_{disp} (m^2 h^{-1}) dispersion coefficient, and F (m) the characteristic length (in this case the bed total height). Curves of tracer concentration in samples as function of time obtained as results from RTD experiments allowed the calculation of variance and average residence time. The Péclet number (Pe) for mass transfer was calculated as $(u_L\,F)/D_{disp}$. Total liquid hold-up, ϕ (m^3) was calculated by multiplying by Q_L. Liquid film depth, L (m) was determined by dividing total liquid hold-up by the biofilm superficial area (a_b).

Biofilm physical features determination

The examination of the biofilm was performed between day 10 and 20 (see Fig. 3). Biofilm volume in PUF was evaluated by extracting five packing pieces from the BTF. Afterwards, the biomass from each piece was individually detached by successive washings and centrifuged to measure pellet volume. An average between all samples was calculated to have a representative value of biomass concentration throughout the BTF. Biofilm thickness (δ) was estimated by dividing the biomass volume by the clean packing superficial area (a_p).

Magnetic resonance imaging (MRI) analysis was applied to some of the colonized packing pieces. For this technique, some carrier cubes were submerged in alkaline mineral medium mixed with gadolinium contrast agent (Gadovist, 1 mmol L^{-1}, Bayer, Mexico). Afterwards, the foam cubes were drained for 1 h and then analyzed in a magnetic scanner (Varian, VNMR 7 T, USA). Gradient echo multi slice (GEMS) sequences were acquired in a 50 per 50 mm field with a 512× 512 pixel matrix giving a resolution of 97.5 μm. Sequences of 80 images were acquired from each cube taking a slice image every 0.5 mm. Only the biofilm structure impregnated with the contrast medium was registered as the polyurethane matrix is invisible in this assay. Superficial area and volume of the biofilm were calculated from 3D reconstructions made with the OsiriX imaging software. Estimates of volume occupied either by total liquid hold-up or biofilm volume were deducted from packing material original void space to have an approximation of the actual bed porosity (ε).

Analytical methods

Biofilm protein content was measured by digestion in 0.2 N NaOH and further analysis with a reagent kit assay (DC BioRad, USA). Gaseous DMDS concentration was analyzed using a gas chromatograph equipped with a FPD detector (HP 5890, USA) and a capillary column (Varian CP-PORABOND Q 25 m×0.32 mm×5 μm, USA). Sulfate was determined according to Standard Methods (1998). Dextran blue liquid concentration was evaluated by spectrophotometry at 290 nm (Jiménez et al. 1988). To evaluate gas treatment performance

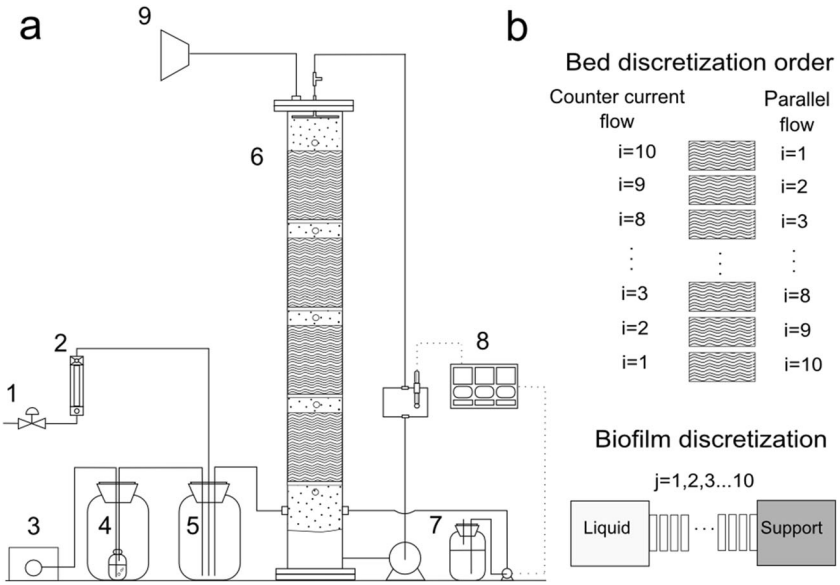

Fig. 1 **a** Diagram of the biotrickling filter for DMDS treatment. *1* Needle valve; *2* rotameter; *3* peristaltic pump; *4* DMDS bubbling vessel; *5* mixing vessel; *6* packed bed; *7* sodium hydroxide 1 N solution; *8* pH control; and *9* exhaust gas extractor. **b** Reactor bed discretization used for modeling

in the BTF, the elimination capacity, EC ($g_{DMDS}\ m^{-3}\ h^{-1}$), and removal efficiency, RE (%), were calculated as:

$$EC = [(C_{in}\text{-}C_{out})/V_{bed}] \times Q_G \quad (3)$$

$$RE = [(C_{in}\text{-}C_{out})/C_{in}] \times 100 \quad (4)$$

Where C_{in} and C_{out} ($g_{DMDS}\ m^{-3}$) are the inlet and outlet concentrations, respectively, Q_G ($m^3\ h^{-1}$) is the gas flow rate, and V_{bed} (m^3) is the packed bed volume.

Biofiltration model

The proposed model is based on the mathematical description of a BTF made previously by Kim and Deshusses (2003). The main assumptions are:

- The packing is completely covered by biofilm, which is in turn entirely coated by a liquid film.
- Gas flow is considered to be plug flow while the axial dispersion model is used for liquid flow.
- Gas-liquid and liquid-biofilm interphases are in equilibrium, according to Henry law constants.
- The biodegradation reaction occurs only in the biofilm and it was not limited by oxygen.

The following partial differential equations describe the dynamic mass balances expressed in concentration (C). Mass balances for oxygen and DMDS (both gaseous and dissolved) and sulfate (dissolved) were calculated in gas, liquid, and biofilm phases considered for BTF modeling. The mass balances for DMDS are depicted in Eqs. 5 to 9. The subscripts G, L, B, and REC denote gas, liquid, biofilm, and recirculation, while iG and iB denote the gas-liquid and liquid-biofilm interfaces, respectively.

Gas phase

$$\frac{\partial C_G}{\partial t} = u_G\frac{\partial C_G}{\partial z} - \frac{k_L a_b}{\varepsilon}[(C_G/H)\text{-}C_L] \quad (5)$$

Where u_G is the gas superficial velocity in the BTF and H is the dimensionless Henry law constant. Initial condition at t=0, C_G=0. Boundary condition at discretization i=1, C_G=C_{in}, either for counter current or parallel flow mode, (see Fig. 1b).

Liquid phase

$$\frac{\partial C_L}{\partial t} = -D_{disp}\frac{\partial^2 C_L}{\partial z^2} + u_L\frac{\partial C_L}{\partial z} + \frac{k_L a_b}{\phi}[(C_G/H)\text{-}C_L] - \frac{a_b D_{eff}}{L}[C_{L(iG)}\text{-}C_{L(iB)}] \quad (6)$$

Where u_L is the superficial liquid velocity inside the BTF. Initial condition at t=0, C_L=0. Boundary conditions for counter current flow C_L=C_{LREC} at i=10. For parallel flow C_L=C_{LREC} at i=1. In any case for i=1 to 10, C_L=C_G/H.

Biofilm

$$\frac{\partial C_B}{\partial t} = \frac{D_{eff}}{\delta^2}\frac{\partial^2 C_B}{\partial x^2} - R_B \quad (7)$$

Where D_{eff} is the diffusion coefficient for DMDS. Initial condition at t=0, C_B=0. Boundary condition at biofilm-liquid

interface j=1, $C_B=C_L$; while at biofilm-support interface $\partial C_B/\partial x=0$.

Biological reaction kinetics

$$R_B = R_{max}\frac{C_B}{C_B + K_S + C_B^2/K_i} \quad (8)$$

The specific rates obtained through respirometry were transformed to volumetric rates in the model considering a ratio of protein to total volume of 0.3 *w/w* of the biofilm in the BTF bed.

Balance for the recirculating liquid at BTF bottom

$$\frac{\partial C_{LREC}}{\partial t} = \frac{Q_L}{V_{LREC}}(C_L - C_{LREC}) \quad (9)$$

Initial condition at t=0, $C_{LREC}=0$.

In order to evaluate the influence of the liquid dispersion over the BTF performance, the model predictions of dispersed flow model were compared with the ideal plug flow, through the inclusion or absence of a dispersion term in the mass balance (Eq. 6).

Model equations were solved with the Matlab® software using the finite differences method. For this procedure, both BTF packed height and biofilm thickness were discretized in ten sections each for simulation (see Fig. 1b). Increasing the discretization number did not change significantly the model estimations.

Polyurethane foam model

The complex internal structure of the polyurethane foam was simplified according to Fig. 2 in order to examine the effect of biofilm growth on superficial area and void space.

The foam, Fig. 2a, was approximated by a tridimensional orthogonal mesh formed by cylindrical PUF filaments as in Fig. 2b. The number and diameter of the filaments in the mesh were adjusted by fitting to the experimentally obtained values of the apparent density (21±0.5 kg m^{-3}) and the filament diameter (0.3±0.1 mm) of the foam used in our assays. The intersections of the filaments (Fig. 2c) implied superficial area and volume losses due to superposition of plastic segments and biofilm. These reductions were accounted in the model considering each node to have the shape of the well-known Steinmetz solid, which is formed by the orthogonal intersection of three cylinders. The area and volume of the Steinmetz solid were calculated as:

$$A_{st} = 3/4\left(16\text{-}8\sqrt{2}\right)D^2 \quad (10)$$

$$V_{st} = \left(2\text{-}\sqrt{2}\right)D^3 \quad (11)$$

Where D corresponds to the diameter of a single filament; the matrix superficial area and volume in a 1 m^3 basis were then calculated as:

$$a_{sp} = (NF\cdot\pi\cdot D\cdot\lambda)\text{-}(3\cdot NI\cdot A_{st}) \quad (12)$$

$$V_{sp} = \left(NF\cdot\pi\cdot 1/4D^2\cdot\lambda\right) - (2\cdot NI\cdot V_{st}) \quad (13)$$

Where NF is the number of filaments, NI is the number of intersections, and λ represents the longitude of filaments, in this case equivalent to 1 m. The effect of biofilm development over the superficial area and biomass volume was evaluated by supposing a uniform biofilm growth on the filaments and thus the diameter in Eqs. 10–13 and Fig. 2c. Biofilm volume estimates were corrected by subtracting the volume of the biofilm-free filament considering the average diameter measured experimentally.

Results

Gas treatment performance in the biotrickling filter

At the beginning of the experiments reported here, the BTF maximum elimination capacity (EC) was 20 $g_{DMDS}m^{-3}$ h^{-1}, with removal efficiency (RE) of around 86 %, as it is shown in

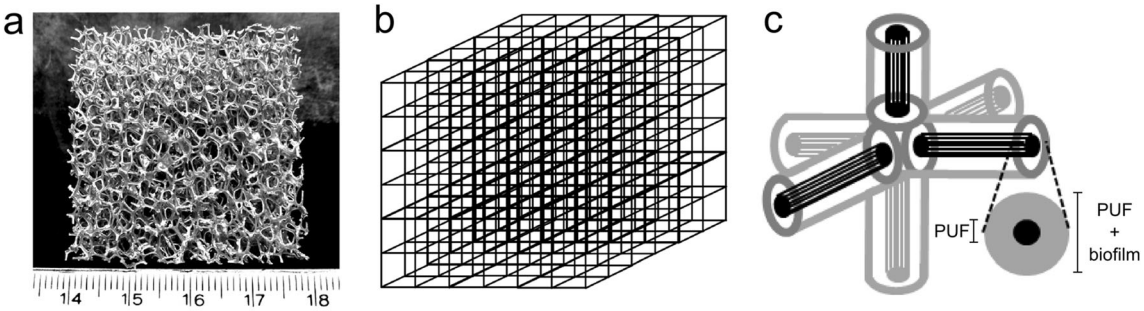

Fig. 2 Photography of the polyurethane foam used in this study, scale below is in centimeters (**a**), basic structure proposed for PUF physical model (**b**), and close up of a three filament intersection covered with biofilm (**c**)

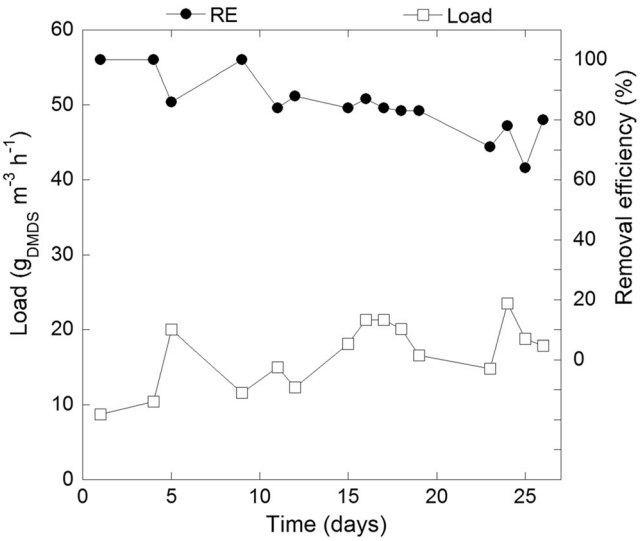

Fig. 3 Biotrickling filter performance evolution during the experimental period. The reactor had been previously operated for over a year

Fig. 3. Concentration of sulfate as the end product of degradation was kept below 10 g L^{-1} to avoid the inhibition on performance previously observed (Arellano-García et al. 2012). The pressure drops were 1.9 and 4.0 cmH_2O m_{column}^{-1} (0.2 and 0.4 kPa m_{column}^{-1}) for parallel and countercurrent mode, respectively.

Polyurethane foam model

Mathematical optimization of the number of filaments in the matrix fitting the experimentally measured packing apparent density of 21±0.5 kg m^{-3} lead to the results presented in Table 1.

With data in Table 1 as the starting point, the superficial area and the volume occupied by the biofilm were estimated using Eqs. 10–13 and varying D which is related to the biofilm depth and the results are depicted in Fig. 4. The irregular bell shape curve predicts initially an increase in the specific area as the biofilm is formed on the filaments by the effect of augmented diameter. As the diameter increases, in this case, beyond a biofilm depth of around 0.7 mm, the superficial area diminishes due to the increment of the node size (Fig. 2c and Eq 12).

Table 1 Estimated properties for the clean polyurethane foam

Parameter	Estimated magnitude
Apparent density of matrix	21 kg m^{-3}
Filament diameter (D)	0.30 mm
Total filaments per meter (NF)	2.55×10^5
Total intersections per meter (NI)	2.49×10^7
Total filaments per linear meter	292
Pores per linear meter	291
Pore size	3.1 mm
Porosity	98 %
Superficial specific area	225 m^2 m^{-3}

Biofilm physical features

Five PUF colonized cubes were sampled between day 10 and 20 (see Fig. 3), and by detaching the biofilm, it was found that 30±2 % of the packed bed volume (0.9 L) was occupied by biomass. After dividing this volume by the superficial area of the clean PUF, an average biofilm thickness of 0.6±0.1 mm was calculated. Further analyses of packing cubes but now with MRI showed a coarse biofilm surface (see Fig. 5) and further image analysis suggested that the biomass occupied approximately 35 % of bed volume while its superficial area was around 650 m^2 m^{-3}. This was similar to the sum of volume percentage calculated by detaching the biomass plus the 2.0 % of the PUF packing volume occupied by polyurethane itself. An animation of the biofilm reconstructed by the MRI images is provided in a video in the Supplementary material section.

Intrinsic biological kinetics

Figure 6 shows the results of the intrinsic oxygen uptake rates from respirometry experiments which were fitted to the reaction model stated in Eq. 8, afterwards the correspondent DMDS consumption kinetics were correlated by using the stoichiometry of Eq. 1. Values of 3,571.6 $g_{DMDS}m^{-3}{}_{biofilm}$ h^{-1}, 2.7 $g_{DMDS}m^{-3}$, and 8.2 $g_{DMDS}m^{-3}$ were determined for R_{max}, K_s, and K_i, respectively.

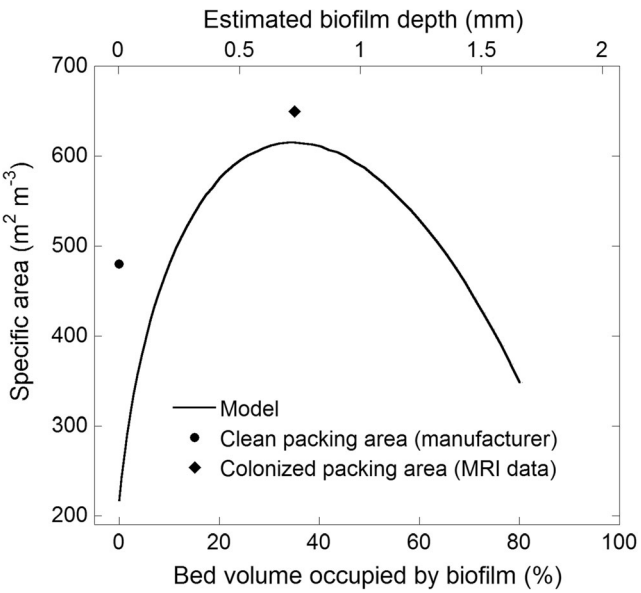

Fig. 4 Specific area volume as functions of biofilm depth, on the model support depicted in Figs. 2b and c

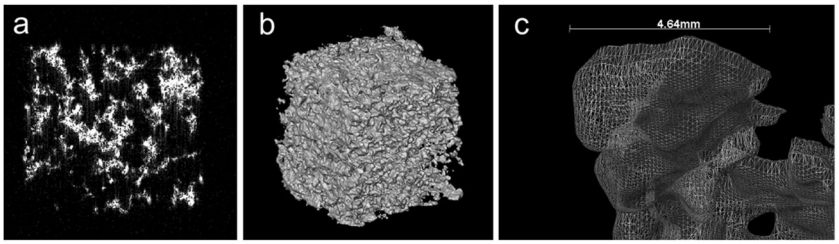

Fig. 5 **a** Original MRI biofilm image in one 4 cm-sided packing cube, **b** 3D reconstruction of biofilm in a packing cube, and **c** close up of a biofilm portion and surface meshing for calculating interfacial area

Trickling liquid flow description

Figure 7 shows the RTD profiles obtained for the liquid flow through the BTF packed bed. It is observed that tracer elution through clean PUF was faster than through colonized PUF maybe as a result of higher liquid hold-up and the tortuosity promoted by biofilm growth. Average liquid residence times through clean and colonized PUF were 10 and 60 s, respectively. In both cases, complete recovery of tracer was verified by mass balances in liquid flow, thus discarding tracer absorption in either biofilm or PUF. By observing the trickling liquid at the bottom of the modules, it was found that biomass growth favors the redistribution of the liquid through the packing.

Main results from RTD experiments for flow through clean and colonized PUF are shown in Table 2. The Péclet number was determined after adjusting the distribution time data to the closed vessel model (Eq. 2).

Biotrickling filter model

Table 3 shows a summary of the parameters introduced in the BTF model for simulate gas treatment. With these parameters, model predictions of concentration profiles with both variations (dispersed and ideal plug flow), either in counter current or parallel flow operation, were compared with experimental data in Fig. 8, where the experimental removal efficiencies were 75 and 80 % for the operation in counter current and parallel mode, respectively. Similar comparison was made with an independent experiment but with an initial concentration of 0.25 g m^{-3} (not shown) with trends similar to those found in Fig. 8.

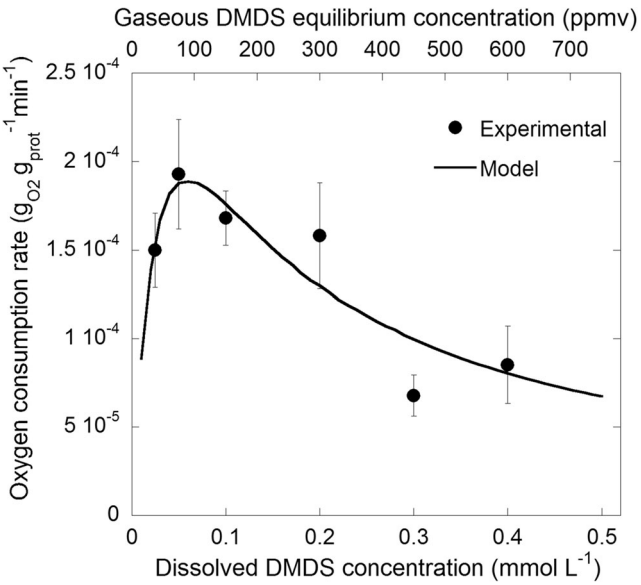

Fig. 6 Alkaline biomass oxygen consumption rates as function of DMDS liquid concentration and fitting to the proposed reaction model (Eq. 8)

Discussion

As it is observed in Fig. 6, results from respirometry fit well a Haldane reaction model with inhibition by substrate. Nonetheless, it is possible to consider that no inhibitory effect of DMDS would be present at the BTF operation conditions reported here, where initial gaseous concentrations never exceeded 140 ppmv (0.54 g m^{-3}). On the contrary, the amount of gaseous DMDS employed in this study promoted liquid concentrations where maximum reaction rate would be located. Compared to kinetics previously reported for DMDS oxidizing bacteria in neutral cultures (Smith and Kelly 1988), the alkaliphilic biofilm in this study showed smaller DMDS affinity and degrading activity of one and two orders of magnitude, respectively. Far from being considered as a drawback, this may imply an advantage for the alkaliphilic

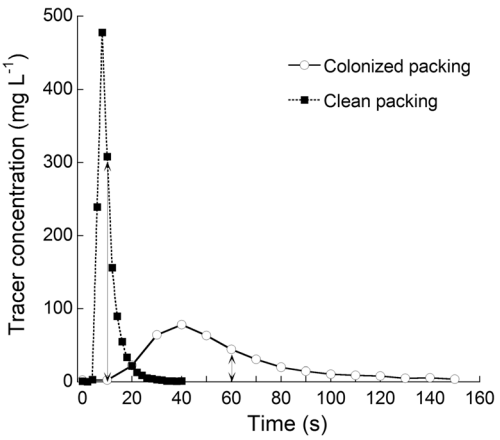

Fig 7 Tracer concentration profiles acquired during DTR experiments. *Vertical arrows* indicate mean residence time

Table 2 Characteristic parameters for liquid flow through packed beds, obtained from RTD experiments

Parameter (units)	Clean PUF	Colonized PUF
Liquid hold up, total (L)	0.1	0.6
Liquid hold up to bed ratio, *v/v* (%)	4	20
Dynamic hold up (L)	0.1	0.3
Liquid film depth (μm)	50	300
Dispersion coefficient (m^2 h^{-1})	0.30	0.72
Péclet number (dimensionless)	10.3	4.3

biomass in biofiltration applications where a slow colonization of packing material would lengthen the time before the appearance of bed channeling or plugging, while microbial activity is enough to carry out low DMDS concentrations removal satisfactorily. In this sense, the observed DMDS elimination capacities during the experiments reported here (Fig. 3) are comparable with the previous reports of DMDS treatment in BTF at neutral pH (Ramirez et al. 2011; Wan et al. 2011). However, it is important to consider that in our case the effective gas residence time was reduced approximately to half of that initially calculated (40 s), due to biomass accumulation and liquid hold-up presence.

In a previous experiment (data not shown), detaching approximately 0.3 L of biomass from the packing lead to an EC increases of nearly 50 %. Nonetheless, it was observed a liquid hold-up increase from 20 to 30 %. The increased elimination capacity obtained in the BTF operation after detaching part of the immobilized biomass may be a consequence of a higher superficial area available for DMDS absorption, nonetheless, this extra area would be equally covered with a trickling liquid film as indicated previously (Picioreanu et al. 2000) explaining the liquid hold-up increase observed after detaching part of the biofilm.

From RTD experiments (Fig. 7), it is seen that biomass accumulation in PUF support leads to an increment of liquid retention time in accordance to results previously reported by other authors (Trejo-Aguilar et al. 2005; Sharvelle et al. 2008a) where the presence of stagnant zones was emphasized. In our case, the intricate porous structure of PUF may influence the liquid flow pattern even when biomass was absent, obtaining Péclet values of 10.3 and 4.3 for liquid flow through clean and colonized PUF, respectively. Having in mind that ideal plug flow is characterized by Pe magnitudes higher than 100 (Levenspiel 1998), it is clear that the dispersion degree is substantial for the liquid flow through PUF at any colonization stage.

As it is portrayed in Fig. 8, the dispersed plug flow model (DPFM) fits better the experimental data than the ideal plug flow model (IPFM), especially when predicting the performance in parallel flow mode. The contrast between DPFM and IPFM shows that dispersion for liquid streams should be considered when modeling BTFs operation, at least when materials similar to open polyurethane foam are used. With respect to the flow mode operation, it was observed experimentally that when BTF was operated in parallel flow mode both smaller liquid hold-up and pressure drop were obtained as compared to counter current flow. This result evidences the interaction between gas and liquid flow direction and suggests that parallel operation may be a better choice at least from the energy consumption point of view. In any case, the biofiltration model predicted that no limitation by oxygen occurred within the biofilm (not shown), although it may not be discarded that actual liquid O_2 concentrations are lower than calculated due to endogenous respiration.

In relation to the real PUF comparison to the mesh model proposed in this study, the main differences arise from the complexity and randomness of real packing, which could promote biomass growth similar to that observed on the MRI images (Fig. 5a, b and Supplementary video). Some PUF estimated properties as average pore size and porosity were in well agreement with measured values. Others, such as

Table 3 Main parameters used in the biofiltration model

Parameter	Value	Reference
DMDS Henry's law dimensionless constant (H)	0.061	Arellano-García et al. 2012
Biofilm thickness (δ)	0.6 mm	This study
Liquid film thickness (L)	0.2 mm	This study
Bed porosity during BTF operation (ε)	0.47	This study
Dispersion coefficient (D_{disp})	0.72 m^2 h^{-1}	This study
DMDS diffusion coefficient (D_{eff})	3.7×10^{-6} m^2 h^{-1}	ICAS
Gas to liquid mass transfer coefficient, liquid side ($k_L a_b$)	26.4 h^{-1}	Bonilla 2013
Biofilm superficial area (a_b)	650 m^2 m^{-3}	This study
Specific max. DMDS uptake rate (R_{max})	3571.6 g m^{-3} biofilm h^{-1}	This study
Saturation constant (K_s)	2.7 g m^{-3}	This study
Inhibition constant (K_i)	8.2 g m^{-3}	This study

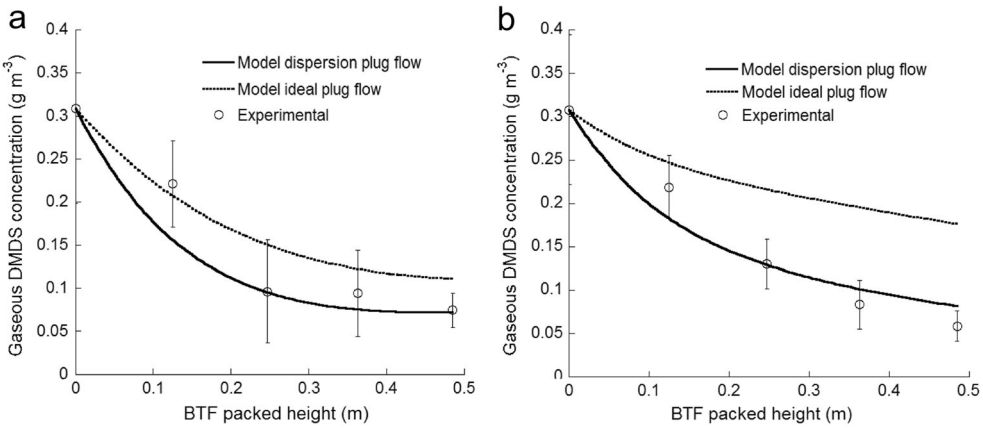

Fig. 8 Experimental and simulated concentration profiles of DMDS along BTF height, for counter current operation (**a**) and cocurrent operation (**b**) for an initial gaseous DMDS concentration close to 0.30 $g_{DMDS} m^{-3}$

the predicted superficial area, were about half of what was reported by the manufacturer. This difference may be attributable to the limitations in the definition and implementation of the relatively simple model and real structure of PUF, in this sense, heterogeneity of filaments width and tortuosity may provide important amounts of superficial area.

Regarding to estimated properties from mesh model, the predicted superficial area for clean PUF was close to 220 $m^2 m^{-3}$ and would rise as a function of biofilm growth until attaining a maximum near 620 $m^2 m^{-3}$, where close to 30 % of packing would be occupied by biomass (Fig. 4). From this point, specific area diminishes as a consequence of further biofilm accumulation. In this respect, a mathematical representation of a biofilter with specific area dependence on biofilm growth was previously reported (Alonso et al. 1998). These authors considered spherical geometry for packing particles and model predictions respecting pollutant removal were in well agreement with experimental data, however, the estimated specific area was invariably decreasing since theoretical biofilm development began. In contrast, the physical model for superficial area utilized in this study led to a bell curve type function (Fig. 4), which fits to scatter data either from foam manufacturer or MRI determination and may serve as evidence of this area tendency actually being happening when PUF is colonized in a biotrickling filter.

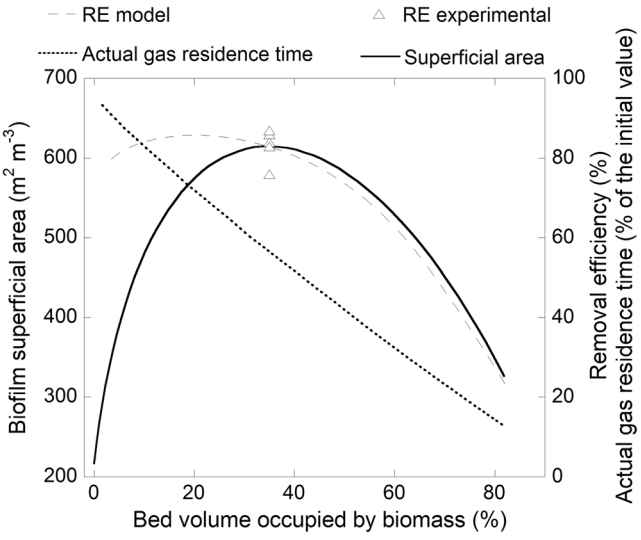

Fig. 9 Theoretical evaluation of biomass accumulation effect over superficial area, removal efficiency (RE) and gas residence time reduction in a BTF treating 27 $g_{DMDS} m^{-3} h^{-1}$, compared to experimental RE data (Δ) at same inlet load

Furthermore, when estimated values of superficial area depicted in Fig. 4 were introduced into the biotrickling filter model, the influence of biomass accumulation over gas residence time and treatment efficiency of the alkaline BTF treating DMDS vapors was estimated and the results are illustrated in Fig. 9.

As shown in Fig. 9, when volume occupied by biomass increased from 0 to 20 %, the specific area also augments from 220 to 570 $m^2 m^{-3}$; nevertheless, RE shows an increment of barely 15 %. This predicted low response in RE when superficial area increases more than 150 % may be a consequence of a process limitation by reaction in biofilm. In this regard, it would be expected that further biomass accumulation lead to higher RE values. Nonetheless, model shows the opposed with an ER drop when biomass attained 32 % of bed volume in spite of area reached 615 $m^2 m^{-3}$. This could be attributable to the gas residence time reduction, which at this point would be 60 % of its initial value. Thereafter, the RE diminishing tendency remains as it is driven by reductions in gas residence time and superficial area.

Images obtained from the MRI analysis showed a biomass structure that agreed with the previous reports (Lewandowski et al. 1995; De Beer and Stoodley 2006) where the biofilm roughness was described. This could lead to superficial area increments and hydrodynamic changes influencing the gas treatment performance in practical applications. In this sense, the biofilm structure effect on mass transport was theoretically addressed by Picioreanu et al. (2000) emphasizing that even when coarseness could lead to a biofilm area rise, effective mass transfer may decrease as only biofilm peaks receive substrate while valleys remain filled with stagnant liquid that hinders substrate diffusion. Therefore, the liquid

velocity through biomass irregularities is highlighted as a determining factor for mass transport through a gas liquid interface. This reasoning could be directly related with experimental evidence in biofiltration applications where liquid flow rate impact over performance was proven in the absence of external mass transfer limitation (Kim and Deshusses 2005).

The agreement between the BTF bed volume occupied by biofilm either evaluated by manually detaching the biofilm or by MRI analysis indicates the possibility of determining some specific parameters with relatively simple procedures. However, further comparisons at different colonized volume fractions and packing materials are required to confirm this evidence.

The theoretical analysis for BTF performance carried out in this study locates the optimum biomass concentration near 20 % of bed volume, which would correspond to a biofilm depth of 0.4 mm immobilized on PUF surface. At this condition, RE close to 90 % would be expected with gas residence time reductions no higher than 30 % (Fig. 9) while pressure drop would be close to 0.5 $cmH_2O\ m_{column}^{-1}$ as it was calculated from the Darcy law equation; this would imply low energy requirements for compressing the gas stream for feeding a biotrickling filter.

In conclusion, the experimental procedures presented in this study were utilized to evaluate parameters which are rarely assessed when colonized supports in a biotrickling filter show extensive microbial growth. These features included gas residence time, superficial area, and dispersion degree in the liquid stream which proved to be closely influenced by biomass accumulation.

With the aid of experimentally determined parameters, the effect of biomass growth on performance of a biotrickling filter was obtained by coupling a simple, yet powerful, representation of the complex PUF topology using an orthogonal mesh to the usual mass balance equations. Model predictions emphasized the relative importance of biotic (such as biomass content and degradative activity) and abiotic (superficial surface, effective residence time, etc.) parameters on performance. Thus, at first stages after startup, modeling predicts biomass concentration to be the biofiltration limiting factor, while at high biomass accumulations, typical of a long-term operation, reduced residence time could determinate the gas treatment efficiency. Furthermore, this theoretical analysis permitted to establish an optimum biomass concentration which could be maintained more easily with a slow growing microbial consortium as alkaliphilic bacteria, while acceptably removal rates of gaseous pollutant would be obtained. It can be predicted that other systems may require less biomass if the specific activity is higher than the consortium used here. Characterization of the biofilm may be performed repeatedly throughout BTF operation to obtain valuable information about the relationship between biofilm growth and gas treatment performance which would be very useful to confirm the viability of representing the complex phenomena occurring inside a BTF by relatively simple models.

Acknowledgements The authors would like to thank Conacyt for financing this project (I0017-166451) and the scholarship of LAG. To AECID for granting the funds for LAG internship in the UPC-Barcelona through project A2/037075/11. And to Rafael Lara and the Ci3M center for MRI analysis.

References

Alonso C, Suidan MT, Sorial GA, Smith FL (1996) Gas treatment in trickle-bed biofilters: Biomass, how much is enough? Biotechnol Bioeng 54(6):583–594

Alonso C, Suidan MT, Kim BR, Kim BJ (1998) Dynamic mathematical model for the biodegradation of VOCs in a biofilter: Biomass accumulation study. Environ Sci Technol 32:3118–3123

Arellano-García L, González-Sánchez A, Van Langenhove H, Kumar A, Revah S (2012) Removal of odorant dimethyl disulfide under alkaline and neutral conditions in biotrickling filters. Water Sci and Technol 66(8):1641–1646

Bonilla WC (2013) Uso de respirometrías heterogéneas para estimar coeficientes de transferencia de masa interfaciales y parámetros biocinéticos en biofiltros de lecho escurrido. Dissertation, UAM Iztapalapa, Mexico

De Beer D, Stoodley P (2006) Microbial biofilms. In: Dwarkin E, Falkow S, Rosenberg E, Schleifer KH, Stackebrandt E (eds) The prokaryotes, 3rd edn. Springer, New York, pp 904–937

Delgado JMPQ (2006) A critical review of dispersion in packed beds. Heat Mass Transfer 42(4):279–310

Deshusses MA, Cox HHJ, Miller DW (1998) The use of CAT scanning to characterize bioreactors for waste air treatment. Paper 98-TA20B.04. In: Proceedings Annual Meeting and Exhibition of the Air and Waste Management Association, San Diego, CA, USA

Dorado AD, Lafuente J, Gabriel D, Gamisans X (2012) Biomass accumulation in a biofilter treating toluene at high loads. Part 2: Model development, calibration and validation. Chem Eng J 209:

Estrada JM, Kraakman NJR, Lebrero R, Munoz R (2012) A sensitivity analysis of process design parameters, commodity prices and robustness on the economics of odour abatement technologies. Biotechnol Adv 30:1354–1363

Gianetto A, Specchia V (1992) Trickle-bed reactors: State of art and perspectives. Chem Eng Sci 47(13):3197–3213

González-Sánchez A, Revah S, Deshusses MA (2008) Alkaline biofiltration of H_2S odors. Environ Sci Technol 42:7398–7404

Granada C, Revah S, Le Borgne S (2009) Diversity of culturable bacteria in an alkaliphilic sulfur-oxidizing microbial consortium. Adv Mat Res 71:137–140

Herskowitz M, Smith JM (1983) Trickle bed reactors: a review. AICHE J 29(1):1–18

Iliuta I, Bildea SC, Iliuta MC, Larachi F (2002) Analysis of trickle bed and packed bubble column bioreactors for combined carbon oxidation and nitrification. Braz J Chem Eng 19(1):69–88

Integrated Computer Aided System (ICAS), Educational Version. Computer Aided Process Engineering Center. Technical University of Denmark

Jiménez B, Noyola A, Capdeville B (1988) Selected dyes for residence time distribution evaluation in bioreactors. Biotechnol Tech 2(2): 77–82

Kim S, Deshusses MA (2003) Development and experimental validation of a conceptual model for biotrickling filtration of H_2S. Environ Prog 22(2):119–128

Kim S, Deshusses MA (2005) Understanding the limits of H_2S degrading biotrickling filters using a differential biotrickling filter. Chem Eng J 113(2):119–126

Levenspiel O (1998) Chemical reaction engineering. John Wiley & Sons, New York

Lewandowski Z, Stoodley P, Altobelli S (1995) Experimental and conceptual studies on mass transport in biofilms. Wat Sci Tech 31(1): 153–162

Neu TR, Manz B, Volke F, Dynes JJ, Hitchcock AP, Lawrence JR (2010) Advanced imaging techniques for assessment of structure, composition and function in biofilm systems. FEMS Microbiol Ecol 72(1):1–21

Picioreanu C, van Loosdrecht MCM, Heijnen JJ (2000) A theoretical study on the effect of surface roughness on mass transport and transformation in biofilms. Biotechnol Bioeng 68(4):355–369

Ramírez M, Fernández M, Granada C, Le Borgne S, Gómez JM, Cantero D (2011) Biofiltration of reduced sulphur compounds and community analysis of sulphur-oxidizing bacteria. Bioresource Technol 102:4047–4053

Sharvelle S, McLamore E, Banks MK (2008a) Hydrodynamic characteristics in biotrickling filters as affected by packing material and hydraulic loading rate. J Environ Eng-ASCE 134:346–352

Sharvelle S, Arabi M, McLamore E, Banks MK (2008b) Model development for biotrickling filter treatment of graywater stimulant and waste gas. I J Environ Eng-ASCE 134:813–825

Silva J, Morales M, Cáceres M, Morales P, Aroca G (2012) Modelling of the biofiltration of reduced sulphur compounds through biotrickling filters connected in series: Effect of H_2S. Electron J Biotechn 15(3):1–15

Smet E, Van Langenhove H (1998) Abatement of volatile organic sulfur compounds in odorous emissions from the bio-industry. Biodegradation 9:273–284

Smith N, Kelly DP (1988) Isolation and physiological characterization of autotrophic sulphur bacteria oxidizing dimethyl disulphide as sole source of energy. J Gen Microbiol 134:1407–1417

Standard Methods for the Examination of Water and Wastewater (1998) 20th edn, American Public Health Association/American Water Works Association/Water Environment Federation, Washington, DC, USA

Trejo-Aguilar G, Revah S, Lobo R (2005) Hydrodynamic characterization of a trickle bed air biofilter. Chem Eng J 113:145–152

Wan S, Li G, An T, Guo B (2011) Co-treatment of single, binary and ternary mixture gas of ethanethiol, dimethyl disulfide and thioanisole in a biotrickling filter seeded with *Lysinibacillus sphaericus* RG-1. J Hazard Mater 186:1050–1057

Zarook SM, Shaikh AA, Azam SM (1998) Axial dispersion in biofilters. Biochem Eng J 1(1):77–84